British Journal of Applied Science & Technology
4(12): 1823-1840, 2014

SCIENCEDOMAIN *international*
www.sciencedomain.org

Study of the Properties of Impulse-Like Pulses in Finite-Difference Time-Domain Simulation of Grounded-Dielectric-Slab-Like Microstrips

Alejandro Dueñas Jiménez[1*]

[1]*Department of Electronics University of Guadalajara, Guadalajara, Jalisco, 44430, Mexico.*

Author's contribution

This whole work was carried by author ADJ.

Original Research Article

Received 30th November 2013
Accepted 17th February 2014
Published 3rd March 2014

ABSTRACT

The study of nine different voltage pulses (exponential, rectangular, unit step, trapezoidal, logarithmic, triangular, quadratic, gaussian, and tangential), which approximate the unit impulse or dirac delta in finite difference time-domain (fdtd) simulation of grounded dielectric slab-like microstrips, was carried out in order to know how each one behaves when transient and steady state analyses are considered. All these pulses lead to almost identical responses (except the unit step) in the frequency regime but to very different performances in the time regime. The convenience of use one pulse instead of other is dicussed on the context of specific applications.

Keywords: Electromagnetic simulation; grounded-dielectric-slab-like microstrips; impulse-like pulses.

1. INTRODUCTION

The propagation speed is a well-defined parameter for totally-confined and semi-confined transmission lines, and also for open transmission lines if the lengthening factor is known and well established. Thus for instance, a simple closed form equation for the phase velocity on a coaxial cable is available in documents everywhere [1,2].

**Corresponding author: E-mail: alejandro.duenas@red.cucei.udg.mx;*

Similarly, an uncomplicated expression to obtain the propagation speed of an open microstrip transmission line, considering the lengthening factor, is at hand in a recent publication [3]. In propagation of pulse signals through transmission lines, two connected aspects of main importance are the transmission line bandwidth, associated with the pulse spectrum (a fast Fourier transform), and the origin of the wave equations, associated with the pulse shape, amplitude and width. The wave equations come from the telegrapher equations, which represent a TEM medium, or from the Maxwell equations, which model TEM and non-TEM media. The pulse shape, amplitude and width come from the summation of several harmonic sine and/or cosine components and a single fundamental (a Fourier series approximation). Thus, although the pulse can be of many different shapes, once it is fed to the transmission line it soon acquires a quasisinusoidal form, since the propagation constant β is a complicated function of the frequency ω (higher order terms in a Taylor series expansion) [4], and because of the spreading of the pulse as it propagates in a dispersive medium [5]. In addition, the voltages and currents in the telegrapher equations, and the electric and magnetic fields in the Maxwell equations, are settled down as continuous-wave cosine-based time-varying variables. Thus, the signal distortion is observed by means of the first and second aspects, whereas the signal change of speed is perceived mainly by way of the second aspect. The propagation speed or phase velocity is the generic name given to the speed with which a constant phase point on a wave displaces. This velocity is the same as the speed of the light for transverse electromagnetic (TEM) media but different (greater or lesser) for non-TEM media where it attains a particular term or designation.

2. THE SIGNAL DISTORTION

The transmission line has a bandwidth which can be defined in terms of the reflection coefficient [6]. These bandwidth determines how much of the spectral content of a certain signal pass throughout the line assigning to it a filtering nature.

In a microstrip transmission line, a hybrid electromagnetic (HEM) non-TEM medium, there are three causes of distortion, as mentioned, one is its filtering nature [6], but also important are its dispersive nature (frequency dependence) [7] and its frequency-shifting nature [3]. If these causes are connected or are a different manifestation of the same phenomenon is something to be carefully studied. The group velocity $v_g = (\partial\beta/\partial w)$ accounts for the dispersive nature in waveguides, but it is identical to the speed of the light, and hence to the phase velocity, for two-conductor or TEM transmission lines [2].

The exponential, unit step, quadratic and Gaussian pulses have only a frequency component, so strictly speaking, they are not distorted. An excellent discussion about the distortion and attenuation of the “wave packets” or pulses carrying the signal information can be found in [8]. A microstrip transmission line is neither a parallel plate waveguide nor a grounded dielectric (slab) waveguide, since a circuital geometry is deposited on the dielectric, partially covering the top overall surface. However, for electromagnetic simulation purposes, mainly when the method of moments (MoM) is being used, an approximated model for the microstrip line may be obtained by considering it like a grounded dielectric slab waveguide [2]. Under these circumstances, a group velocity can be associated to a microstrip with meaningful results. Thus, for the dielectricand air regions of a grounded-dielectric-slab-like microstrip, the propagation constants are given as.

3. THE PHASE AND GROUP VELOCITIES

A microstrip transmission line is neither a parallel plate waveguide nor a grounded dielectric (slab) waveguide, since a circuital geometry is deposited on the dielectric, partially covering the top overall surface. However, for electromagnetic simulation purposes, mainly when the method of moments (MoM) is being used, an approximated model for the microstrip line may be obtained by considering it like a grounded dielectric slab waveguide [2].

Under these circumstances, a group velocity can be associated to a microstrip with meaningful results. Thus, for the dielectric and air regions of a grounded-dielectric-slab-like microstrip, the propagation constants are given as

$$\beta_d = (\varepsilon_d k_0^2 - k_{cd}^2)^{1/2} = (\varepsilon_d (w/c)^2 - k_{cd}^2)^{1/2} \quad (1)$$

$$\beta_a = (k_{ca}^2 + k_0^2)^{1/2} = (k_{ca}^2 + (w/c)^2)^{1/2} \quad (2)$$

where εd is the relative permittivity of the dielectric, k_0 is the magnitude of the free space wavenumber vector resulting from a general plane wave solution of wave equation [2], k_{cd} and k_{ca} are the cutoff wavenumbers for the dielectric and air regions respectively, $\omega = 2\pi f$ is the radian frequency and c is the speed of the light in free space. The sign of k_{ca}^2 in (2) has been chosen to fulfill an exponential decay for the air region and the same propagation constant has been initially assumed for both regions in order to reach a phase matching at the air-dielectric interface, although it remains as the same only for frequencies lesser than a relative low value, as will be seen later. By applying the proper boundary conditions to the solutions of the grounded-dielectric-slab wave equations, and by combining the cutoff wavenumbers, two sets of simultaneous transcendental equations can be arranged for the transverse magnetic (TM) and transverse electric (TE) modes in the following way [2]:

$$k_{cdtm}^2 \tan(k_{cdtm} d) = \varepsilon_d k_{catm} \quad (3)$$

$$k_{cdtm}^2 + k_{catm}^2 = (\varepsilon_d - 1) k_0 \quad (4)$$

$$-k_{cdte} \cot(k_{cdte} d) = k_{cate} \quad (5)$$

$$k_{cdte}^2 + k_{cate}^2 = (\varepsilon_d - 1) k_0 \quad (6)$$

where d is the thickness of the dielectric substrate.

From (1) and (2) the group velocity for each region is given by

$$v_{gd} = c\beta_d / \varepsilon_d k_0 = c/(\varepsilon_d)^{1/2} \, \beta_d/(\varepsilon_d)^{1/2}/k_0 \quad (7)$$

$$v_{ga} = c\beta_a / k_0 \quad (8)$$

Likewise, the phase velocities on the dielectric, the air and the microstrip, uncorrected and corrected are given respectively as [3], [9]

$$v_{pd} = c/(\varepsilon_d)^{1/2} \quad (9)$$

$$v_{pa} = c \quad (10)$$

$$v_{pm} = c/(\varepsilon_{eff})^{1/2} = c1/(\varepsilon_{eff})^{1/2} = cv_{rp} \quad (11)$$

$$v_{pmc} = v_{pmfl} = v_{pm}\, kv^{n}_{pm} / v^{n}_{pd} \quad (12)$$

where ε_{eff} is the effective dielectric constant, v_{rp}, is the relative phase velocity, fl is the lengthening factor, k and n are positive numbers and $k = p/2$ (where p is the number of circuit ports).

Now then, from (1) it can be seen that k_{cd} is real only if $k_0 > \beta_d/(\varepsilon_d)^{1/2}$ and from (2) k_{ca} is real only if $\beta_a > k_0$.

Hence $v_{gd} < v_{pd} < v_{pm} < v_{pmc} < v_{pa} = v_{ga}$ since $(\varepsilon_d)^{1/2} \geq 1$ and $(\varepsilon_{eff})^{1/2} > 1$. For a microstrip line with a relative permittivity of 10.5, a substrate thickness of 0.0635 *cm* and a strip width of 0.1882 *cm* (a characteristic impedance of approximately 25 Ω), this sequence is complied only for frequencies below 2.8131 GHz, where the phase matching is reached. For frequencies over this value, TM dielectric v_{gdtm} an air v_{gatrm} group velocities fluctuate among underluminal and superluminal values and TE counterparts have the constant values of $v_{gdte} = 2.8552 \times 10^{7}$ and $v_{gate} = c$.

Likewise, the air and dielectric TM and TE group velocities have a relationship given by

$$v_{gdtm} = \varepsilon_{dvgdtm} \quad (13)$$

$$v_{gdte} = \varepsilon_{dvgdte} \quad (14)$$

This behavior is confirmed by the results shown on Figs. (1) to (11). Obviously, the results given by (1)-(8) are valid only for one dimensional time-harmonic waves but not for two- and three- dimensional waves, which require a plane scalar wave equation in vector space to describe the wave movement [10].

A group velocity has only significance if the bandwidth of the signal pulse is relatively small. This requires a Fourier series approximation composed solely by harmonic components constrained to a narrow band around the fundamental frequency [8] and demand a modulating or intelligent signal with a very low frequency as compared to the frequency of the carrier signal ($w_m << w_0$). However, the surface waves on a grounded dielectric slab [11] can propagate even at optical frequencies (THz) where an intelligent signal may have a considerable bandwidth [12].

From 3.07 to 3.09 GHz, a cumulus of adjacent superluminal speeds coinciding with a dispersed and purely imaginary propagation constant can be observed on Figs. (1), (4) and (6). The origin of this heap may be the fact that they are in the neighborhood of an infinite propagation constant and group velocity located at 3.0822 GHz.

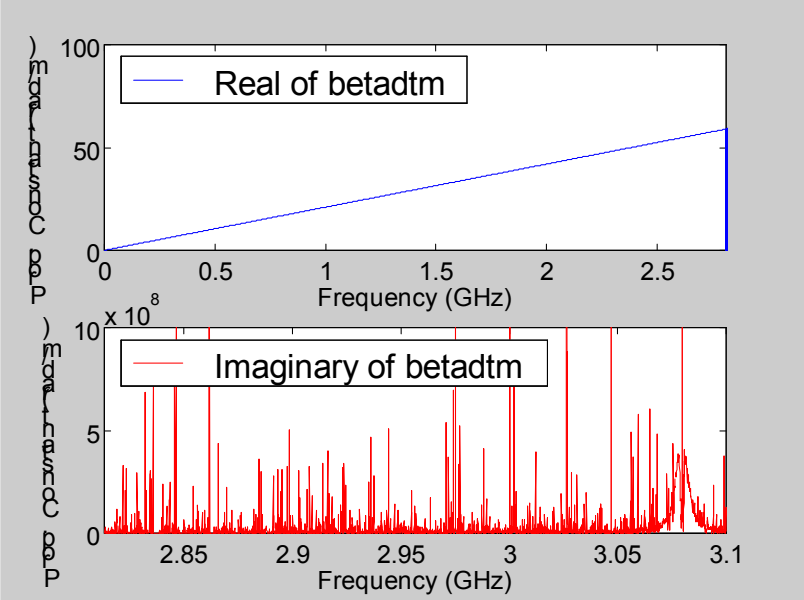

Fig. 1. The dielectric TM mode propagation constant growing with frequency. It remains purely real from 0 to 2.8131 GHz and then pass to a fluctuation from real to imaginary

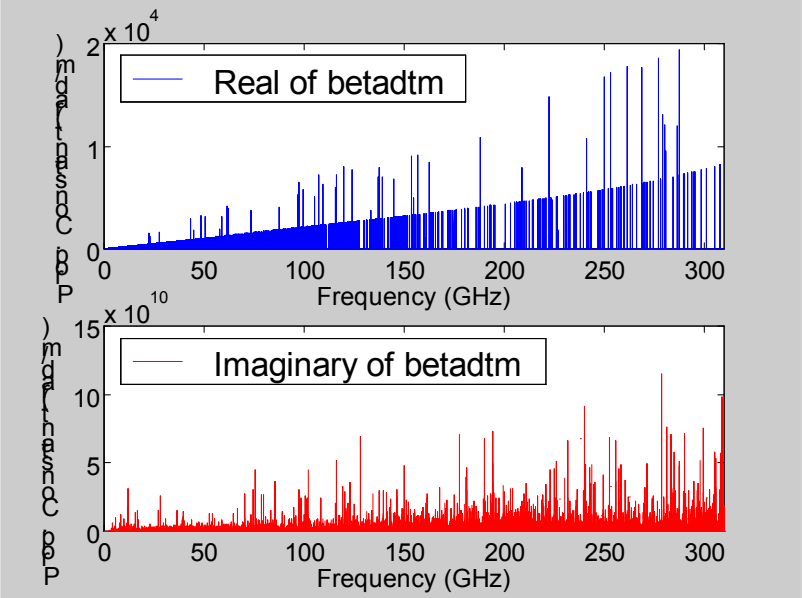

Fig. 2. Behavior of the dielectric TM mode propagation constant at higher frequencies. A sustained exponential growth is beheld on the real part

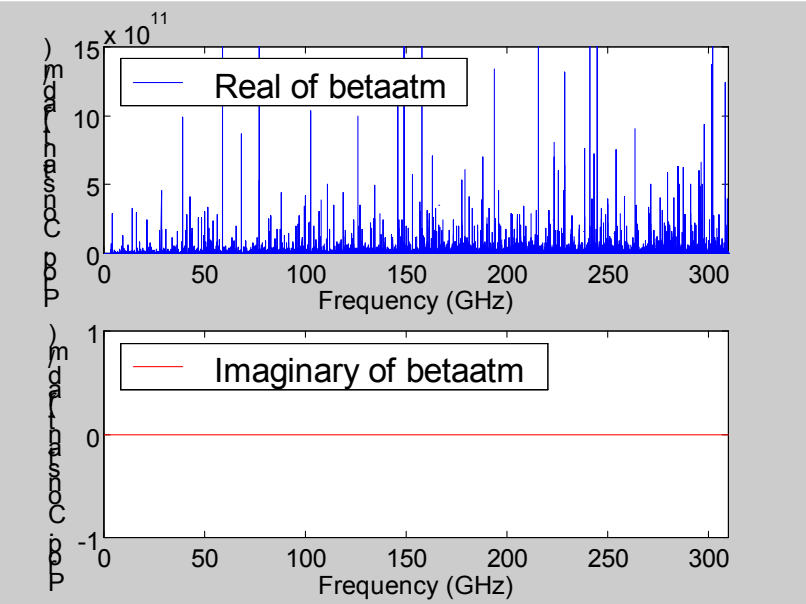

Fig. 3. Behavior of the air TM mode propagation constant at higher frequencies. The imaginary part becomes 0

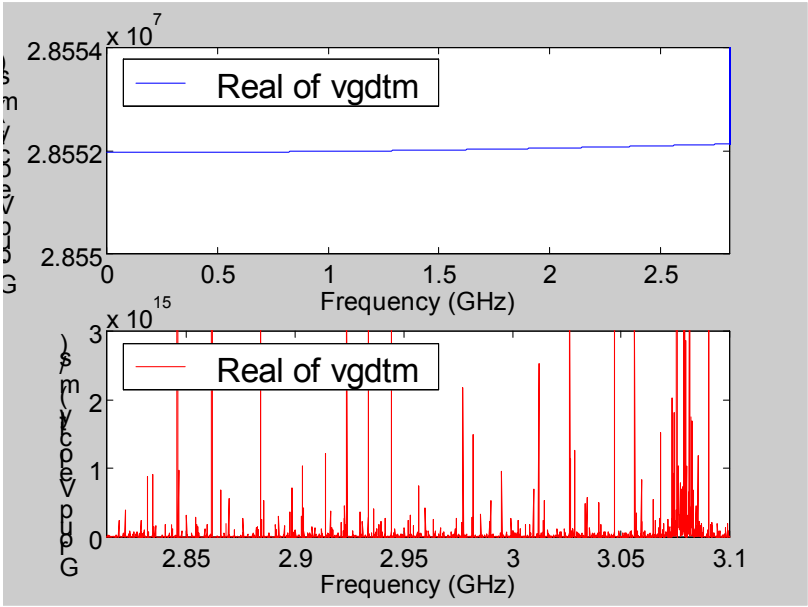

Fig. 4. The dielectric TM mode group velocity flying from underluminal to superluminal speeds in a narrow band. A small deviation from a constant can be observed from 0 to 2.8131 GHz

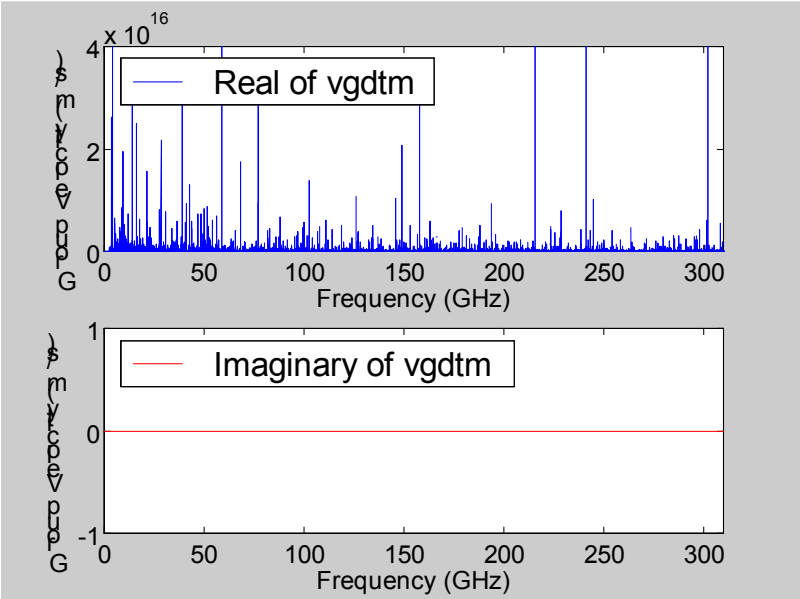

Fig. 5. The dielectric TM mode group velocity flying from underluminal to superluminal speeds in a wide band. The imaginary part becomes 0

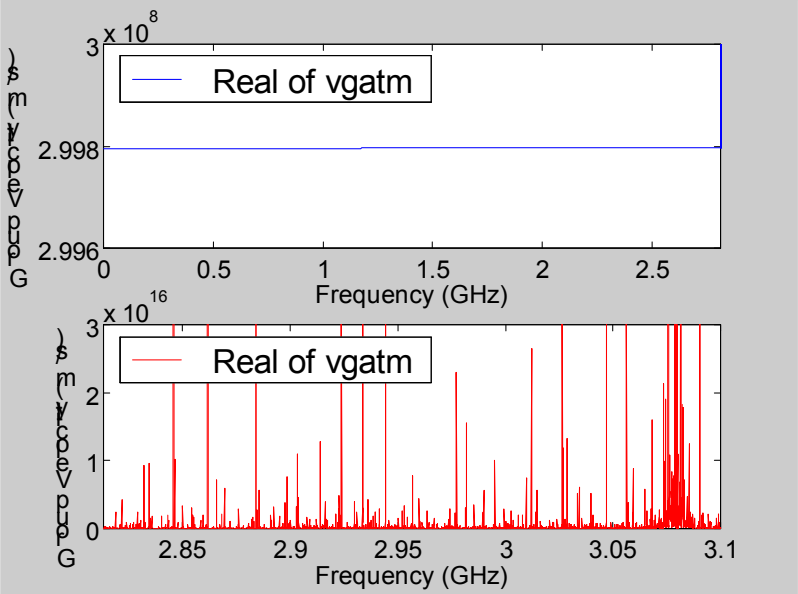

Fig. 6. The air TM mode group velocity flying from luminal to superluminal speeds in a narrow band. The free-space speed of light remains unchanged until 2.8131 GHz

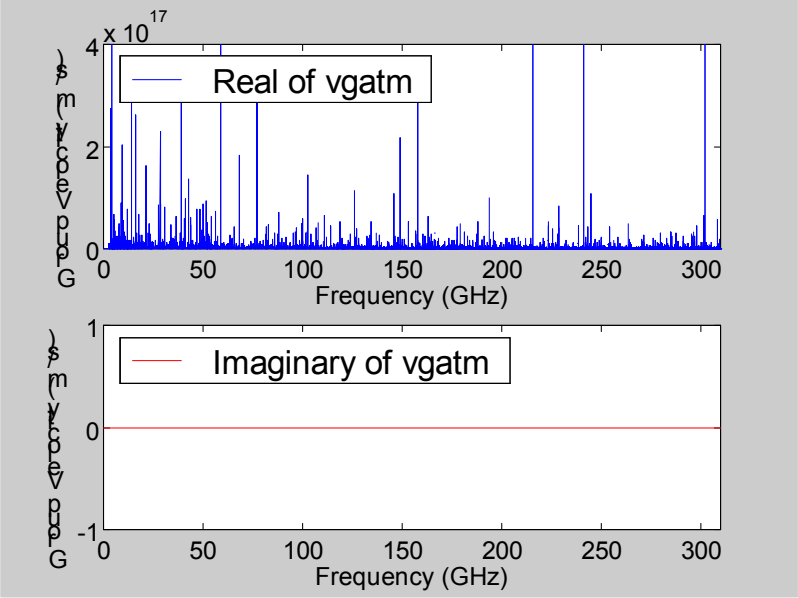

Fig. 7. The air TM mode group velocity flying from luminal to superluminal speeds in a wide band. The imaginary part becomes 0

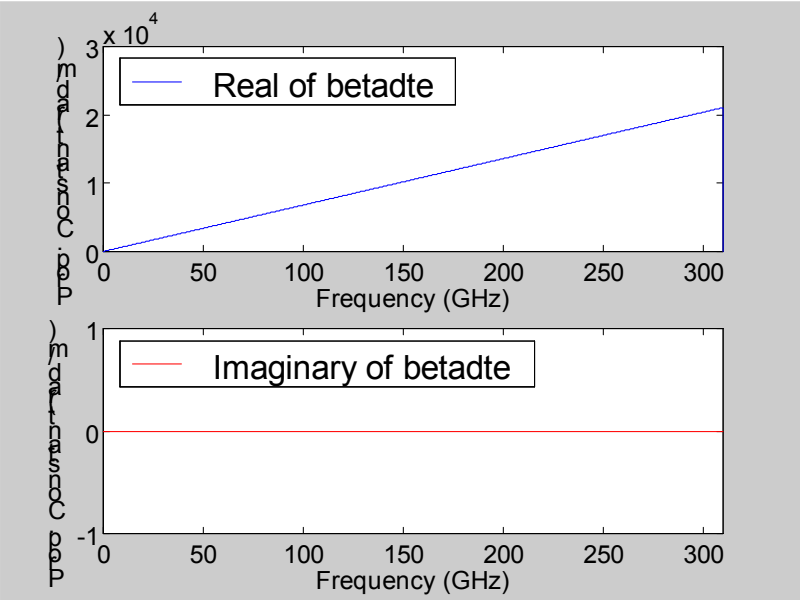

Fig. 8. Behavior of the dielectric TE mode propagation constant at higher frequencies. A simple constant growth is beheld on the real part and the imaginary part becomes 0

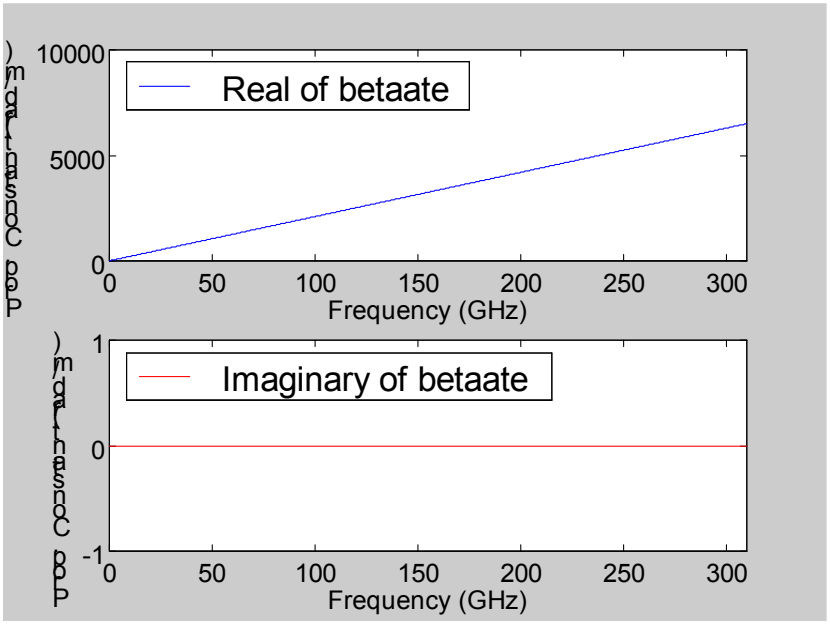

Fig. 9. Behavior of the air TE mode propagation constant at higher frequencies. A simple constant growth is beheld on the real part and the imaginary part becomes 0

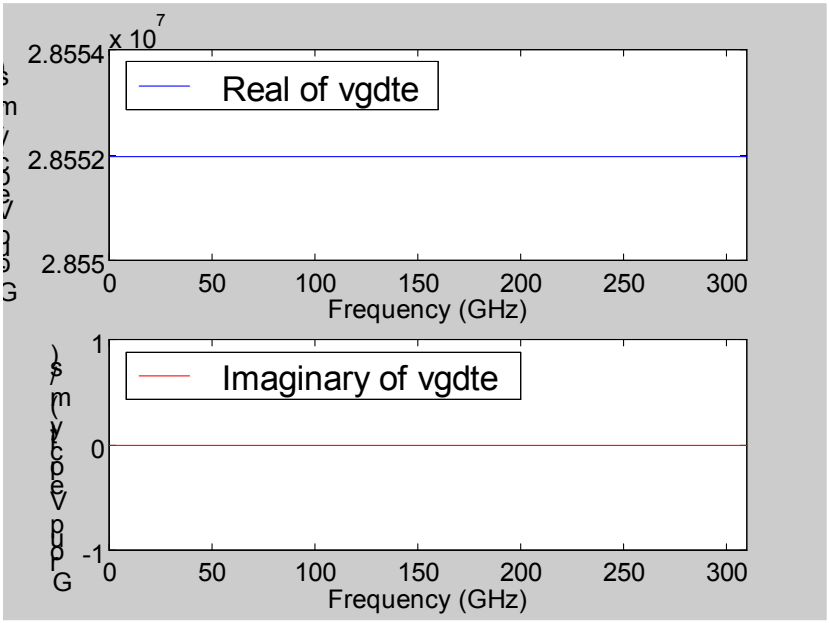

Fig. 10. The dielectric TE mode group velocity showing a wide band underluminal flat behavior. The imaginary part becomes 0

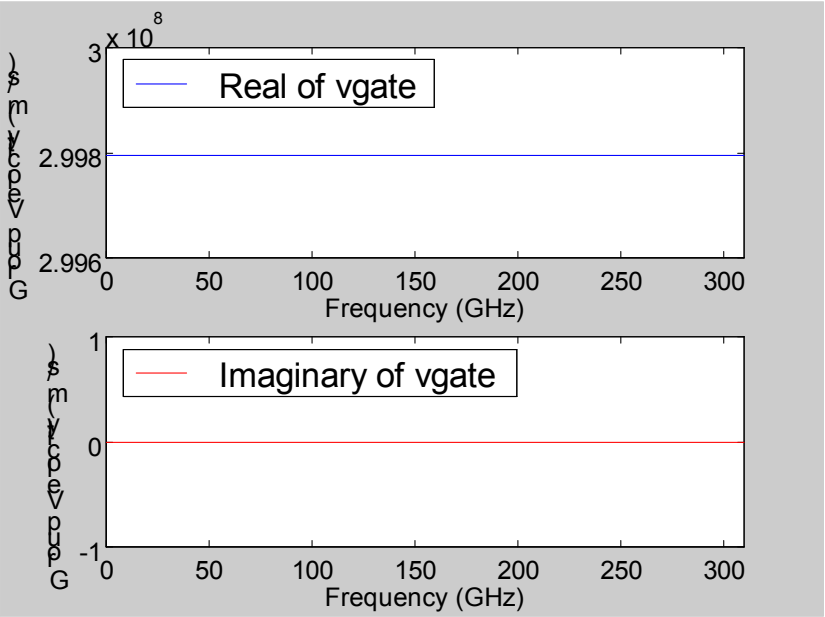

Fig. 11. The air TE mode group velocity showing a wide band luminal flat behavior. The imaginary part becomes 0

4. PULSE DEFINITION AND IMPLEMENTATION

Typically, a pulse is defined by a multivariable function including parameters as the pulse shape, the pulse amplitude and the pulse width or spread .However, if the signal has a simple geometrical shape, an easier way to define and implement a pulse is by using logical conditions as simple Matlab® code statements [13]. The nine voltage pulses are defined as follows:

Exponential (logical condition):

$$pulse = \left(0.5e2 * \exp\left(-t\right)\right).*\left(abs\left(t >= 0 \ \& \ t <= 20\right)\right); \tag{15}$$

Rectangular (logical condition):

$$pulse = 2.5 * \left(abs\left(t >= 0 \ \& \ t <= 20\right)\right); \tag{16}$$

Unit step (logical condition):

$$pulse = 2.5 * \left(abs\left(t >= 0 \ \& \ t <= T\right)\right); \tag{17}$$

where T is a summation incrementing by one inside the main loop of a 2-D FDTD electromagnetic simulation [9],

Trapezoidal (logical condition):

$$\begin{aligned} pulse = {} & (0.2 * t).*(abs(t >= 0 \ \& \ t <= 10)) \\ & + 2.0 * (abs(t > 10 \ \& \ t <= 30)) \\ & + (8.0 - 0.2 * t).*(abs(t > 30 \ \& \ t <= 40)); \end{aligned} \tag{18}$$

Logarithmic (logical condition):

$$pulse = \log(t).*(abs(t >= 0 \ \& \ t <= 20)); \tag{19}$$

Triangular (logical condition):

$$\begin{aligned} pulse = {} & (0.2 * t).*(abs(t >= 0 \ \& \ t <= 20)) \\ & + (8.0 - 0.2 * t).*(abs(t > 20 \ \& \ t <= 40)); \end{aligned} \tag{20}$$

Quadratic (logical condition):

$$pulse = (1.5e-2 * t.\hat{}\ 2).*(abs(t >= 0 \ \& \ t <= 20)); \tag{21}$$

Gaussian (function):

$$pulse = 3 * \exp(-(0.5 * ((20 - t)\hat{}\ 2) / (spread\ \hat{}\ 2))); \tag{22}$$

where $spread$ is taken as 4.

Tangential (logical condition):

$$\begin{aligned} pulse = {} & (1.0 / (8.0 - 1.5e-2 * t.\hat{}\ 2)) \\ & .*(abs(t > 20 \ \& \ t <= 40)); \end{aligned} \tag{23}$$

Figs. (12) to (20) show the fast Fourier transforms, the stimulated microstrip transmission line input impedances and the elapsed one-way travel times for each one of the proposed pulses. From a comparison of the responses, curves and traces shown in these figures, it can be realized that the Gaussian pulse has the cleanest shape since not appreciable wake is leaved behind it. However, compared to other pulses, the Gaussian pulse is one of the slower pulses, meaning a greater computer memory and a time-consuming computation is required for long paths and high speed interconnects simulations. On the other hand, the exponential pulse has a fast transit time with a very noticeable trail which however, can be reduced by applying a larger $spread$ as mentioned in [14]. The other pulses are intermediate cases where one instead of other can be chosen on the basis of design and simulation criteria. Thus for instance, the trapezoidal pulse is an appropriate one to perform frequency- and time-domain simulations for crosstalk minimization. Table I shows a comparison among voltage pulses presenting the time of flight to reach the end of a microstrip line with dimensions as those given in the previous section.

Table 1. Comparison among voltage pulses

Pulse	Cell at which the maximum value (mean) of the pulse appears at 168 time steps (C_m)	Time steps required to the mean reaches the cell 51 (end of the line)	Elapsed time to the mean reaches the cell 51 (sec)
Exponential	51	168	2.8978e-10
Rectangular	50	171	2.9495e-10
Unit Step	49	174	3.0013e-10
Trapezoidal	48	177	3.0530e-10
Logarithmic	48	177	3.0530e-10
Triangular	47	180	3.1048e-10
Quadratic	47	180	3.1048e-10
Gaussian	46	184	3.1738e-10
Tangential	44	191	3.2945e-10

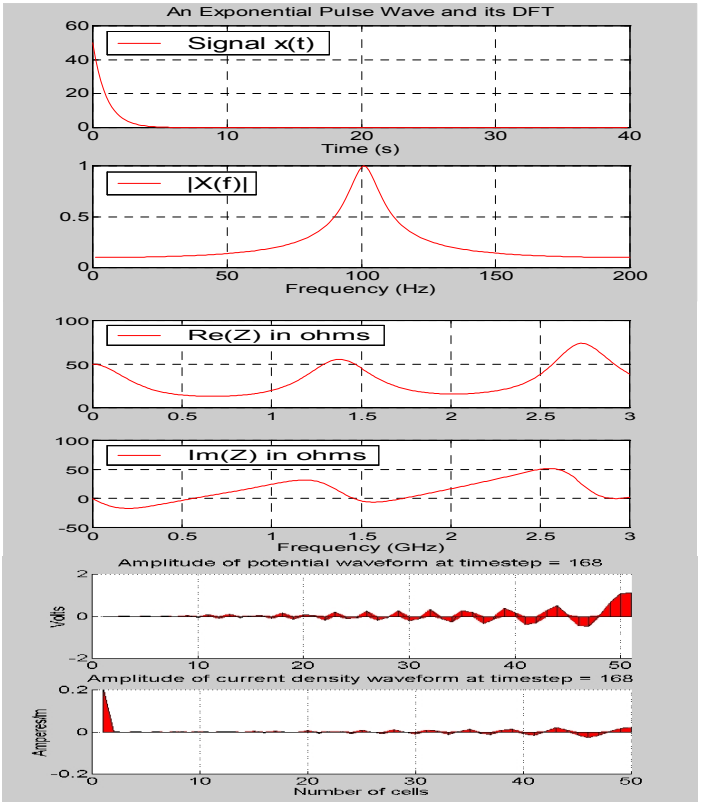

Fig. 12. The fast Fourier transform of an exponential pulse wave. The input impedance of a microstrip transmission line when is stimulated by an exponential pulse wave. Elapsed time necessary for the mean of an exponential pulse wave reaches the cell 51 (sec)

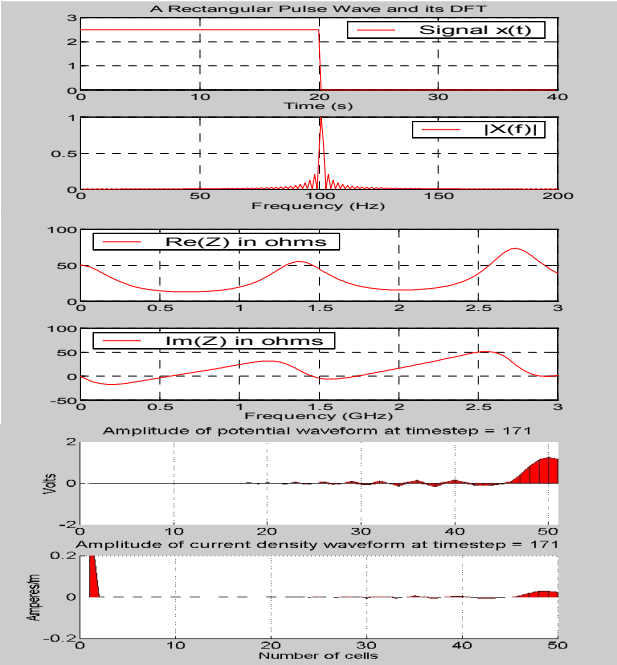

Fig. 13. The fast Fourier transform of a rectangular pulse wave. The input impedance of a microstrip transmission line when is stimulated by a rectangular pulse wave. Elapsed time necessary for the mean of a rectangular pulse wave reaches the cell 51 (sec)

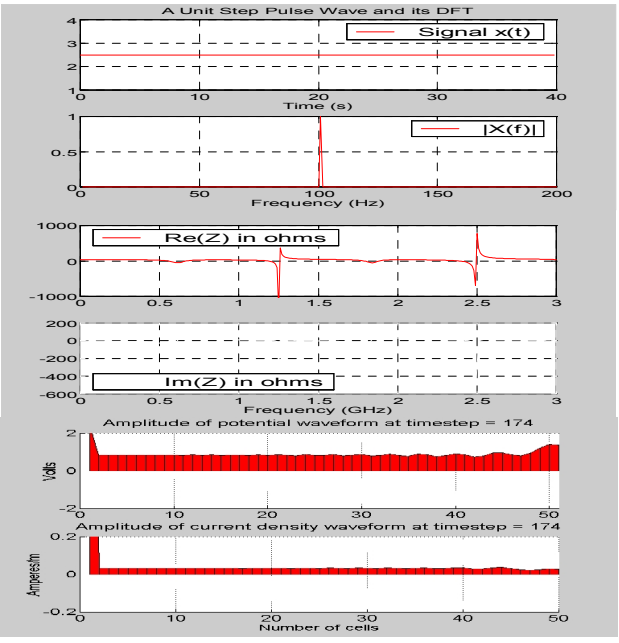

Fig. 14. The fast Fourier transform of a unit step pulse wave. The input impedance of a microstrip transmission line when is stimulated by a unit step pulse wave. Elapsed time necessary for the mean of a unit step pulse wave reaches the cell 51 (sec)

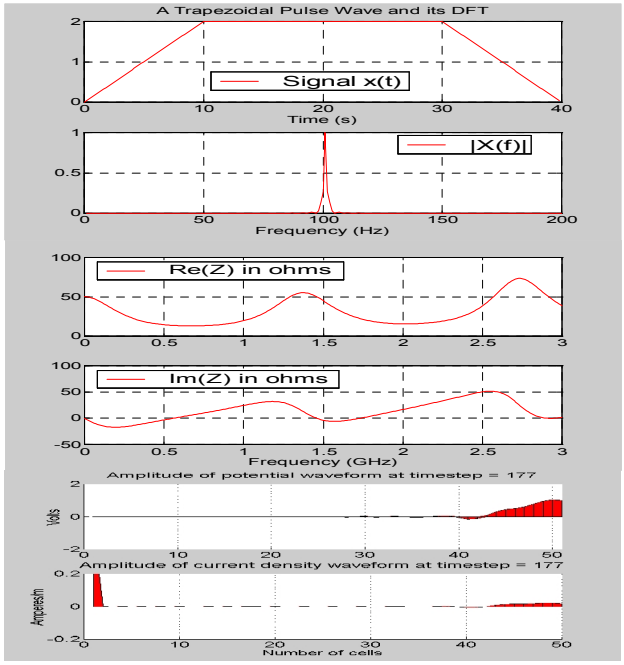

Fig. 15. The fast Fourier transform of a trapezoidal pulse wave. The input impedance of a microstrip transmission line when is stimulated by a trapezoidal pulse wave. Elapsed time necessary for the mean of a trapezoidal pulse wave reaches the cell 51 (sec)

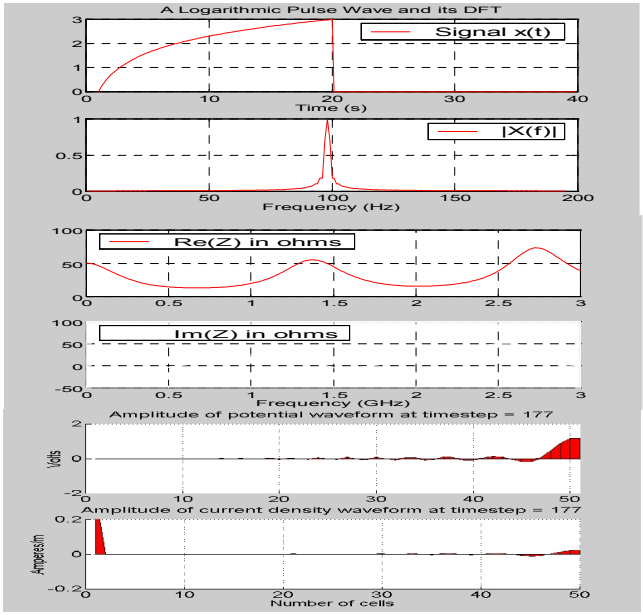

Fig. 16. The fast Fourier transform of a logarithmic pulse wave. The input impedance of a microstrip transmission line when is stimulated by a logarithmic pulse wave Elapsed time necessary for the mean of a logarithmic pulse wave reaches the cell 51 (sec)

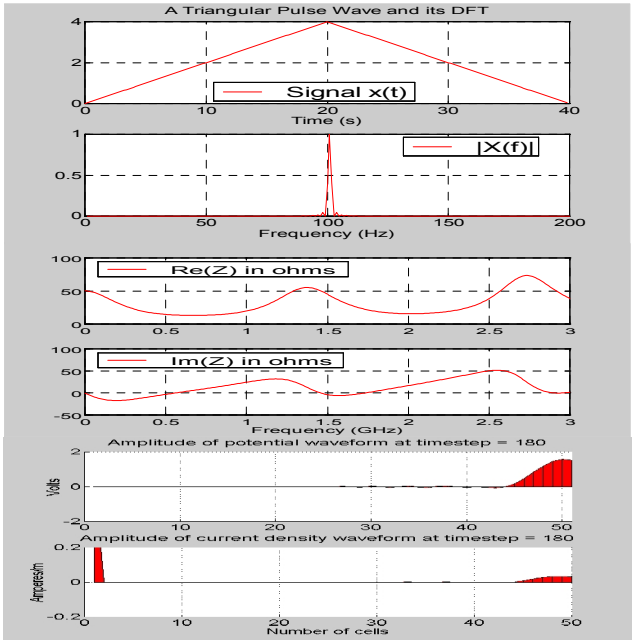

Fig. 17. The fast Fourier transform of a triangular pulse wave. The input impedance of a microstrip transmission line when is stimulated by an exponential pulse wave. Elapsed time necessary for the mean of an exponential pulse wave reaches the cell 51 (sec)

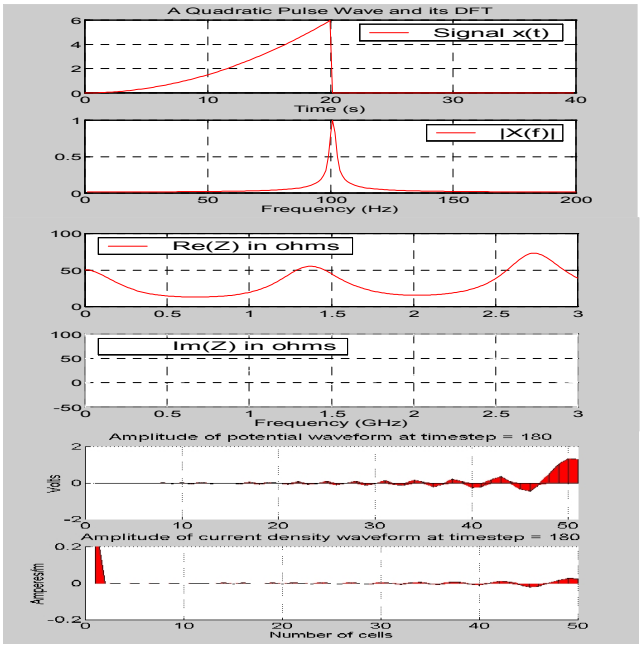

Fig. 18. The fast Fourier transform of a quadratic pulse wave. The input impedance of a microstrip transmission line when is stimulated by a quadratic pulse wave. Elapsed time necessary for the mean of a quadratic pulse wave reaches the cell 51 (sec)

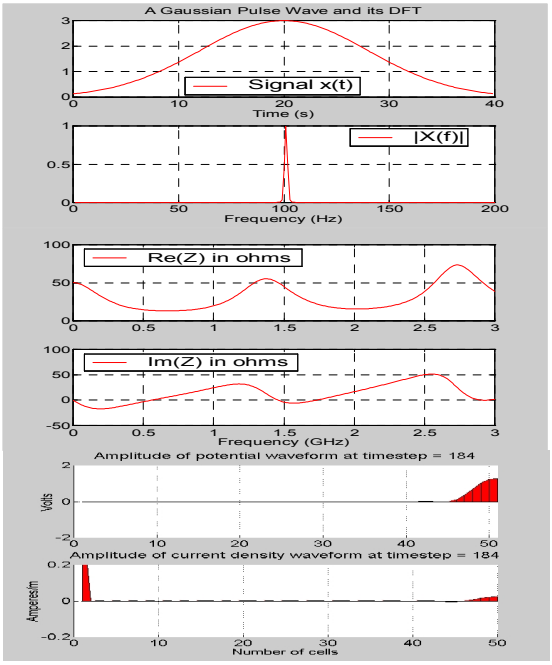

Fig. 19. The fast Fourier transform of a Gaussian pulse wave. The input impedance of a microstrip transmission line when is stimulated by a Gaussian pulse wave. Elapsed time necessary for the mean of a Gaussian pulse wave reaches the cell 51 (sec)

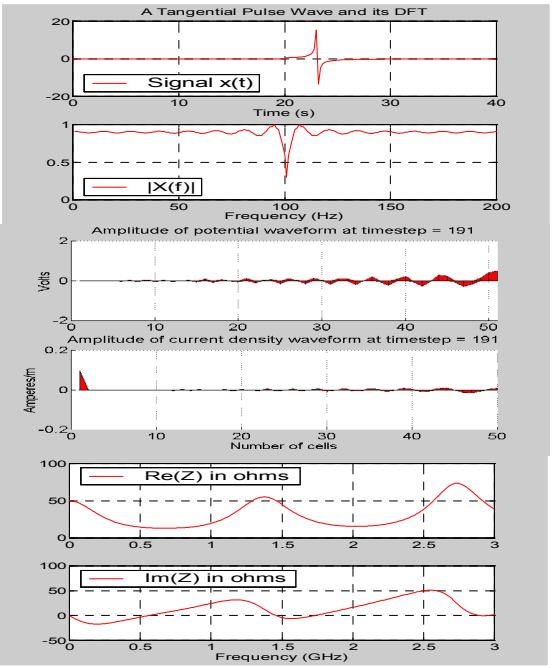

Fig. 20. The fast Fourier transform of a tangential pulse wave. The input impedance of a microstrip transmission line when is stimulated by a tangential pulse wave. Elapsed time necessary for the mean of a tangential pulse wave reaches the cell 51 (sec)

5. CONCLUSION

A study of nine pulses or wave packets to stimulate microstrip transmission line circuits, as paths and high speed interconnects, was carried out in order to know how they behaves in both the transient and steady state regimes. The microstrip wave velocities were deduced by considering the distortion as the result of three phenomena of distinctive nature: the filtering nature, the dispersive nature and the frequency-shifting nature. The pulses were defined by a mathematical function or by a code logical condition. As an important corollary it can be noted that the transit time for each pulse is substantially different.

COMPETING INTERESTS

Author has declared that no competing interests exist.

REFERENCES

1. Collin RE. Foundations for Microwave Engineering, New York: McGraw-Hill; 1992.
2. Pozar DM. Microwave Engineering, Reading, Massachusetts: Addison-Wesley; 1990.
3. Dueñas Jiménez A. Frequency- and time-domain simulation of microstrip squares by using 2D-FDTD electromagnetic analyses. Int. Journal Microw. Opt. Tech. 2010;5:1-6.
4. Elliot RS. An Introduction to Guided Waves and Microwave Circui*ts*, New Jersey: Prentice Hall. 1993;103-109.
5. Jackson JD. Classical Electrodynamics, New York: John Wiley & Sons. 1999;326-329.
6. Przedpelski AB. Bandwidth of transmission line matching circuits. Microwave Journal. 1978;71-76.
7. Getsinger WJ. Microstrip dispersion model, IEEE Trans. Microwave Theory Tech., vol. MTT-21. 1973;34-39.
8. Stratton JA. Electromagnetic Theory, New York: McGraw-Hill. 1941;301-309:330-333.
9. Dueñas Jiménez A. 2-D Electromagnetic Simulation of Passive Microstrip Circuits, Boca Raton, FL: CRC Press a Taylor and Francis Company. 2009;274. Gong M, Jeon T, Grischkowsky D. THz surface wave collapse on coated metal surfaces. OSA Optics Express. 2009;17:17088-17101.
10. Shin CS, Nevels R. Optimizing the Gaussian pulse excitation function in the finite difference time domain method. IEEE Trans. Educ. 2002;45:15-18.
11. Cohen E, Sharma B, Barnes M. Observation of the effects of the Fourier transformation on Periodic Signals. ECE 521. Project 2, Computer Vision & Image Processing Lab. University of Louisville, Kentucky. USA; 2007.
12. Dueñas Jiménez A. Practical criteria for the implementation of a hybrid FDTD-MoL technique used for electromagnetic analysis of microstrip paths. IEICE Electronics Express. 2010;7:58-66.13.
13. Zhang ZM, Park K. On the group front and group velocity in a dispersive medium upon refraction from a nondispersive medium. Transactions of the ASME. 2004;126:244-249.

14. Davalos Guzmán U, Dueñas Jiménez A. Graphical exegesis of the TE and TM surface waves on a stratified microstrip. To be published in the 53rd IEEE International Midwest Symposium on Circuits and Systems, Seattle, Washington; 2010.

Peer-review history:
The peer review history for this paper can be accessed here:
http://www.sciencedomain.org/review-history.php?iid=445&id=5&aid=3875